



## Diurnal-seasonal and weather-related variations of land surface temperature observed from geostationary satellites

Konstantin Y. Vinnikov,<sup>1</sup> Yunyue Yu,<sup>2</sup> M. K. Rama Varma Raja,<sup>3</sup> Dan Tarpley,<sup>2</sup> and Mitchell D. Goldberg<sup>2</sup>

Received 22 August 2008; revised 6 October 2008; accepted 9 October 2008; published 29 November 2008.

[1] The time series of clear-sky Land Surface Temperatures (LST) for one year, 2001, obtained from pyrgeometric observations at five selected US surface radiation (SURFRAD) stations and independently retrieved for the locations of these stations from Infrared Imager hourly observations of two geostationary satellites, GOES-8 and GOES-10, are presented as a sum of time-dependent expected value (diurnal and seasonal cycles), and weather-related anomalies. The availability of three independent observations is used to assess random and systematic errors in LST data. Temporal variation of the expected value is approximated as a superposition of the first two annual and diurnal Fourier harmonics. This component of temporal variations of LST absorbs all systematic errors; which themselves are often a subject of diurnal and seasonal variations. The results revealed that the weather-related temporal variation of LST is much smaller than the temporal variations of the expected value, but much larger than the random errors of observation. Scale of temporal autocorrelation of weather-related component of clear-sky LST variations is about 3 days. **Citation:** Vinnikov, K. Y., Y. Yu, M. K. Rama Varma Raja, D. Tarpley, and M. D. Goldberg (2008), Diurnal-seasonal and weather-related variations of land surface temperature observed from geostationary satellites, *Geophys. Res. Lett.*, 35, L22708, doi:10.1029/2008GL035759.

### 1. Introduction

[2] Sea Surface Temperature (SST) monitoring using infrared observations from NOAA satellites is relatively easy because SST is spatially homogeneous, with a weak diurnal cycle and slow temperature variations. However, the Land Surface Temperature (LST) is spatially inhomogeneous, with a very large diurnal cycle and a strong dependence on cloudiness. As such, the monitoring of LST is extremely difficult. Compared to the polar orbiting satellites, the geostationary satellites provide an opportunity for monitoring the diurnal variation of LST at each location. Even though infrared measurement of the land surface temperature from a satellite is possible only for cloudless sky, such monitoring is an important component of the GOES satellites observational program [Schmit *et al.*, 2005]. While the spatial resolution of current geostationary

infrared radiometers is somewhat lower than for polar orbiters, the higher temporal frequency of observations on a continuous monitoring basis makes these measurements highly valuable. Radiance measurements using split window IR channels (centered near 11  $\mu\text{m}$  and 12  $\mu\text{m}$ ) are ideal for determining LST under clear conditions because of the small correctable water vapor absorption [McMillin, 1975; McMillin and Crosby, 1984; Yu *et al.*, 2008].

[3] Let us define clear-sky LST as temperature  $T(t|_{c=0})$ , where  $t$  is time, and the  $c = 0$  condition means that cloudiness  $c(t)$  at the time of observation  $t$  is equal to zero. This temperature does not exist at the time of observation  $t|_{c \neq 0}$  with cloudy sky. The largest components of the temporal variation of clear-sky LST is its diurnal and seasonal cycles which is given by time-dependent expected value. The expected value is estimated here using only one year of data so that it represents observations over one particular (reference) year and can therefore be biased. The residual fluctuations are interpreted as the “weather-related” component of clear-sky LST variability. The observed LST is also contaminated by systematic and random errors. The main goal of this research is a quantitative statistical assessment of diurnal/seasonal and weather-related components of observed variations of clear-sky land surface temperature, and associated observational errors.

### 2. Data

[4] The coincident LST data sets used in the current study contain clear-sky hourly observations from the GOES-8 and GOES-10 satellites and measurements from five Surface Radiation Budget SURFRAD, stations (Table 1) for the year 2001. The determination of cloudy versus clear-sky conditions over the SURFRAD site locations is manually determined using a cloud screening technique [Rama Varma Raja *et al.*, 2008].

[5] In the current study, the SURFRAD measurements are considered as “ground truth”. The LST values are computed using the Stefan-Boltzmann law together with the observed upwelling and downwelling IR (3  $\mu\text{m}$  to 50  $\mu\text{m}$ ) irradiance measurements, calibrated to broad-band fluxes. The broadband emissivities are obtained from Snyder *et al.* [1998]. The available data are three-minute averages of infrared fluxes. Downward looking pyrgeometers are positioned at 8 meters above the land surface so that the measured radiation fluxes at each one of the SURFRAD sites are hemispheric in nature.

[6] For match-up of the satellite and SURFRAD observed data the following criteria are adopted: (1) The satellite pixel should be the one closest to the SURFRAD site within the GOES field of view (FOV). (2) Since the

<sup>1</sup>Department of Atmospheric and Oceanic Sciences, University of Maryland, College Park, Maryland, USA.

<sup>2</sup>NESDIS/NOAA, Camp Spring, Maryland, USA.

<sup>3</sup>I. M. Systems Group, Inc., NESDIS/NOAA, Camp Spring, Maryland, USA.

**Table 1.** List of Selected SURFRAD Stations With Their Coordinates and Statistics<sup>a</sup>

SURFRAD Station Name	Satellite Field of View Vegetation Type		Location		Number of Observations	Annual Mean, $a_{00j}$ °C			Standard Error			COR			Systematic Error, $\Delta_{i,j}$ °C		
	Lat°N	Lon°W	Lat°N	Lon°W		$i = 1$	$i = 2$	$i = 3$	$\delta_j$ °C	$\delta_2$ °C	$\delta_3$ °C	$r_{i,2}$	$r_{i,3}$	$r_{2,3}$	$\Delta_{2,1}$	$\Delta_{3,1}$	$\Delta_{3,2}$
Goodwin Creek, MS	34.25	89.87	34.25	89.87	510	14.3	14.3	13.0	0.6	0.8	0.7	.96	.97	.96	0.7	-0.2	-0.9
Desert Rock, NV	36.63	116.02	36.63	116.02	3190	21.5	19.7	19.9	0.6	1.2	0.8	.92	.94	.90	-2.3	-2.0	0.3
Bondville, IL	40.05	88.37	40.05	88.37	1160	9.5	11.2	9.2	1.3	0.8	0.8	.92	.92	.96	0.3	-1.2	-1.6
Boulder, CO	40.13	105.24	40.13	105.24	1350	10.8	10.4	9.6	0.9	1.3	1.0	.94	.95	.93	-0.7	-1.1	-0.4
Fort Peck, MT	48.31	105.10	48.31	105.10	1360	6.2	5.9	5.1	1.1	1.1	0.8	.96	.97	.97	-0.5	-0.9	-0.4

<sup>a</sup>Numbers of used observations coincident in time at SURFRAD stations, GOES-8 and GOES-10 satellites; annual mean LST  $a_{00j}$ ; standard errors of LST observation  $\delta_j$ ; standard deviation  $\sigma$  of weather-related component of LST; correlation between residuals of LST approximation, COR ( $r_{i,j} = Y_i - Y_j$ ); mean differences  $\Delta_{ij}$  between nighttime observed LST. Index  $i, j = 1, 2, 3$  means: 1 - SURFRAD station, 2 - GOES-8, and 3 - GOES-10 satellite observation.

SURFRAD observations are provided every 3-minutes, the GOES data should be matched to the closest SURFRAD time within the 3-minute interval. It must be noted that there is a 15-minute shift between hourly observations from the two satellites.

[7] The LST values are derived from GOES-8 and GOES-10 observations using a split window algorithm originally developed by *Ulivieri and Cannizzaro* [1985] and modified by *Yu et al.* [2008]. The modification includes a path length correction term to take into account the varying path length as a function of satellite view zenith angle. Land type-dependent surface emissivities are obtained from *Snyder et al.* [1998].

**3. Method**

[8] Observed temporal variations of the observed meteorological variable  $y(t)$ , where  $t$  is time, can be expressed as a sum of the time-dependent expected value  $Y(t)$ , the weather-related anomaly  $y'(t)$  and the random error of observation  $\varepsilon(t)$ :

$$y(t) = Y(t) + y'(t) + \varepsilon(t). \tag{1}$$

We are going to estimate systematic diurnal/seasonal variations in the observed data  $y(t)$ , standard deviations and lag-correlation functions of weather-related anomalies, and standard errors of observations.

**3.1. Approximation of Diurnal-Seasonal Cycles in Observed LST**

[9] The mathematical model used for approximation of the time-dependent expected value  $Y(t)$  is the same as that was used by *Vinnikov and Grody* [2003] and *Vinnikov et al.* [2004, 2006], but without the trend component:

$$Y(t) = \sum_{k=-K}^K \sum_{n=-N}^N a_{kn} e^{i2\pi t(\frac{k}{T} + \frac{n}{H})}. \tag{2}$$

The function  $Y(t)$  in (2) is expressed as the product of two finite series of Fourier harmonics of annual ( $T = 1$  year) and diurnal ( $H = 1$  day) cycles. At least the first two harmonics of annual and diurnal periods ( $N = K = 2$ ) must be used to correctly describe the seasonal and diurnal variation in the expected value  $Y(t)$ . The unknown coefficients  $a_{kn}$  can be estimated using the least square technique, assuming randomness of weather-related anomalies  $y'(t)$  and independence of errors  $\varepsilon(t)$ .

**3.2. Estimation of Standard Errors of Observations**

[10] Considering three independent observations of clear-sky land surface temperature at the location of a SURFRAD station, from (1) we can write:

$$\begin{aligned} y_1(t) - Y_1(t) &= y'(t) + \varepsilon_1(t), \\ y_2(t) - Y_2(t) &= y'(t) + \varepsilon_2(t), \\ y_3(t) - Y_3(t) &= y'(t) + \varepsilon_3(t). \end{aligned} \tag{3}$$

It is known from observation, that LST simultaneously observed from different directions may be different [*Minnis and Khaiyer*, 2000]. This is why  $Y_1(t) \neq Y_2(t) \neq Y_3(t)$ . The weather-related component of LST variation  $y'(t)$  in (3) is,

by definition, the same for all three observations. We also assume that  $y'(t)$  and random errors  $\varepsilon_1(t)$ ,  $\varepsilon_2(t)$ , and  $\varepsilon_3(t)$  are uncorrelated. There are many different physical sources of errors in each of these integral errors. Each of them includes random error of the radiometer, of calibration, of surface emissivity, of the split window technique, of the footprint spatial averaging, of satellite footprint position and many others. But, we have to limit our desire to characterize each single source of random errors and try to interpret their integral. The independence of random errors gives us an opportunity to estimate unknown variances of weather-related signal and random errors

$$\sigma^2 = \overline{(y')^2}, \delta_1^2 = \overline{(\varepsilon_1)^2}, \delta_2^2 = \overline{(\varepsilon_2)^2}, \delta_3^2 = \overline{(\varepsilon_3)^2}. \quad (4)$$

Let us find differences of each pair of the equations (3) and then apply an operator of variance, VAR, to both sides of the obtained expressions. This yields a system of three equations to estimate three unknown standard errors  $\delta_1$ ,  $\delta_2$ ,  $\delta_3$ .

$$\begin{aligned} \text{VAR}[y_1(t) - Y_1(t) - y_2(t) + Y_2(t)] &= \delta_1^2 + \delta_2^2, \\ \text{VAR}[y_2(t) - Y_2(t) - y_3(t) + Y_3(t)] &= \delta_2^2 + \delta_3^2, \\ \text{VAR}[y_3(t) - Y_3(t) - y_1(t) + Y_1(t)] &= \delta_3^2 + \delta_1^2. \end{aligned} \quad (5)$$

### 3.3. Variances and Lag-Correlations

[11] Each single equation of (3) can be used to estimate the variance  $\sigma^2$  of weather-related anomalies of LST:

$$\begin{aligned} \sigma^2 &= \text{VAR}[y_1(t) - Y_1(t)] - \delta_1^2 = \text{VAR}[y_2(t) - Y_2(t)] - \delta_2^2 \\ &= \text{VAR}[y_3(t) - Y_3(t)] - \delta_3^2. \end{aligned} \quad (6)$$

For each of the stations we can obtain the time series of this variable  $y'(t)$ , but contaminated by random errors of observation,  $y'(t) + \varepsilon_1(t) = y_1(t) - Y_1(t)$ ,  $y'(t) + \varepsilon_2(t) = y_2(t) - Y_2(t)$ , and  $y'(t) + \varepsilon_3(t) = y_3(t) - Y_3(t)$ . Assuming that these random errors are statistically independent of the weather-related signal,  $\overline{y'(t_1)\varepsilon_i(t_2)} = 0$  for arbitrary  $t_1$  and  $t_2$ , and not correlated in time,  $\varepsilon_i(t_1)\varepsilon_i(t_2) = 0$  for  $t_1 \neq t_2$ , we can use each of the observed time series of LST  $y_i(t)$ ,  $i = 1, 2, 3$ , to evaluate lag-correlation functions  $R(\tau)$ , where  $\tau$  is lag, of weather-related signal  $y'(t)$ .

$$\begin{aligned} R_i(\tau \neq 0) &= \text{COV}([y_i(t) - Y_i(t), y_i(t + \tau) - Y_i(t + \tau)]) \\ &/ [(\sigma^2 + \delta_i^2)/\sigma^2], R_i(\tau = 0) = 1. \end{aligned} \quad (7)$$

## 4. Diurnal-Seasonal and Weather-Related Variations of Clear-Sky LST and Errors

### 4.1. Diurnal-Seasonal Variations

[12] Let us use the following indices for observations of LST at SURFRAD station location: “1” for the station observation, “2” for the GOES-8 observation, and “3” for the GOES-10 observation. Observations made during the same  $\sim 15$ -min time intervals are considered to be “simultaneous”. For each of the selected SURFRAD stations we have a time series of independently observed LST which are

$y_1(t)$ ,  $y_2(t)$  and  $y_3(t)$ . These time series have been approximated with expression (2) using an ordinary least squares technique. The estimated coefficients in (2) give us an opportunity to compute time-dependent expected (reference year) values  $Y_1(t)$ ,  $Y_2(t)$  and  $Y_3(t)$  for an arbitrary  $t$ . The time-dependent expected value of LST can be displayed as a function of two different times, the time interval from the beginning of a day, and the time interval from the beginning of a year. The estimates of seasonal and diurnal variations of clear-sky LST obtained from observation at five selected SURFRAD stations  $Y_1(t)$  are shown in the first column of panels in Figure 1. They are very large, several tens of  $^\circ\text{C}$ , significantly larger than seasonal and diurnal variations of surface air temperature, not shown here. This is the systematic component of LST variation. It is expected that seasonal and diurnal variation varies very slowly from year to year, assuming the ground cover remains the same.

### 4.2. Systematic Differences and Random Errors

[13] Differences between estimates  $Y_1(t)$ ,  $Y_2(t)$  and  $Y_3(t)$  are almost indistinguishable visually, but they can be clearly seen in the plots for these differences,  $Y_2(t) - Y_1(t)$ ,  $Y_3(t) - Y_1(t)$  and  $Y_3(t) - Y_2(t)$ , that are presented in Figure 1. These differences have significant seasonal and diurnal cycles. The relatively small observational plots beneath the land-based station radiometers are always horizontal and homogeneous. But, a combination of (1) slopes of different orientation, (2) sometimes very complicated topography and landscapes within a satellite footprint, and (3) surface shadowing, are responsible for significant angular anisotropy of a temperature field. Let us look, for example, at the estimates of systematic differences between LST in the vicinity of the Desert Rock SURFRAD station as observed by GOES-8 and GOES-10. This difference is relatively small at nighttime and during winter months when the sun is low. But, during the summer months, LST observed by GOES-8 (located at  $75^\circ\text{W}$ ) in the morning hours after sunrise is a few degrees larger than LST observed by GOES-10 (located at  $135^\circ\text{W}$ ); and *vice versa*, LST observed by GOES-10 in the afternoon is a few degrees larger than LST observed by GOES-8. The sign of the difference depends on the relative sun-satellite azimuth angles and the value of this difference depends on zenith angle of the sun. Thermal inertia smoothes and delays expected temperature changes.

[14] Much larger differences can be observed in the regions of intensive agricultural activity where LST measurements at SURFRAD stations are not representative for much larger satellite footprints. We see such a phenomenon in the estimated differences of  $Y_2(t) - Y_1(t)$  and  $Y_3(t) - Y_1(t)$  for the Bondville, IL, SURFRAD station. Satellite-observed LST in the vicinity of this station is affected by soil cultivation in the spring time and by crop harvesting in autumn. Real, but relatively small, systematic errors of the instruments are included in these large physical effects. Expected values of LST,  $Y_1(t)$ ,  $Y_2(t)$ ,  $Y_3(t)$  and their differences should be evaluated and taken into account, if data from surface stations and satellites are going to be used together for LST monitoring. Information on vegetation types in the satellite field of view for SURFRAD stations is given in Table 1. Description of land cover in the field of

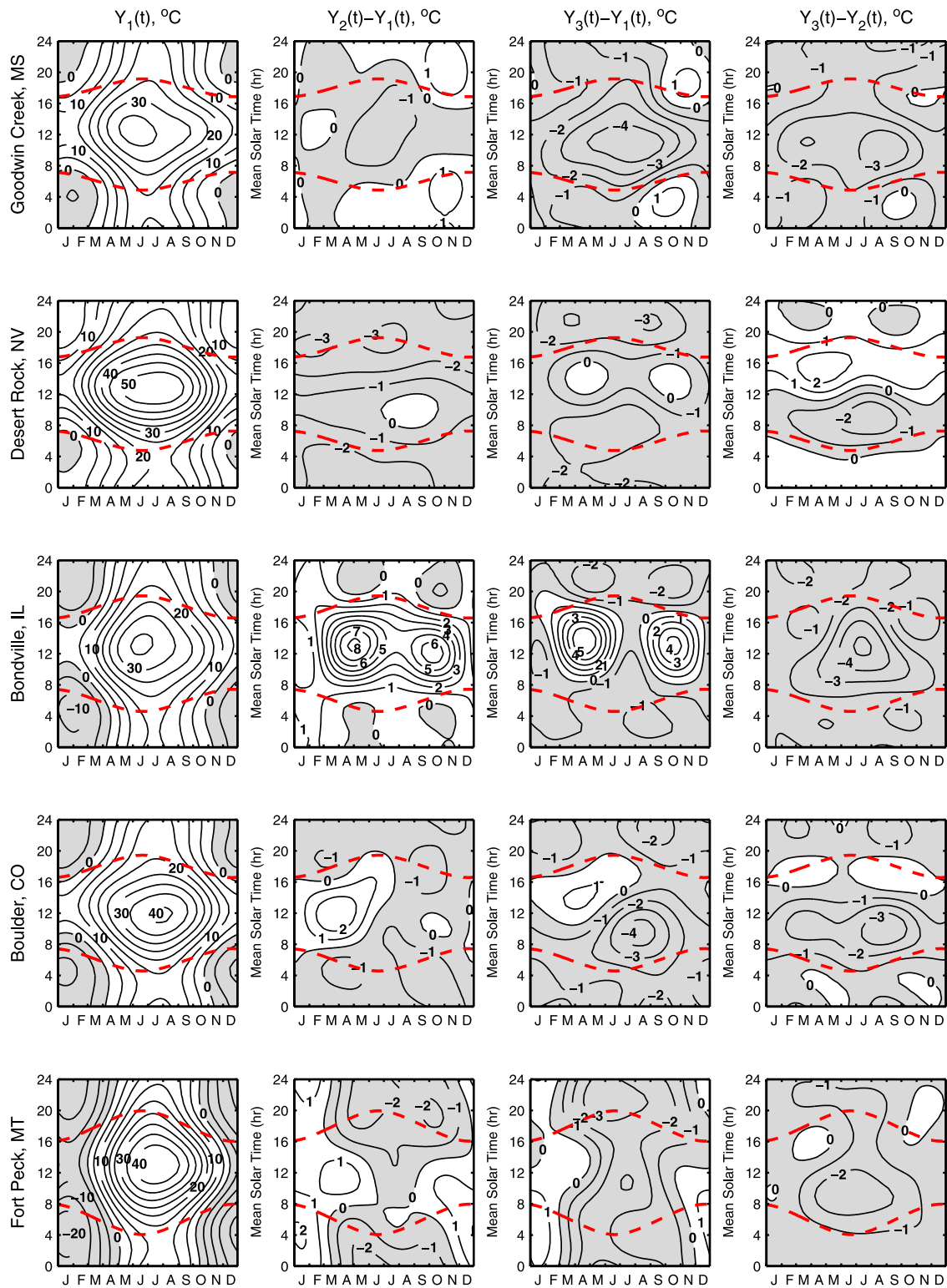


**Figure 1.** Estimates of seasonal and diurnal variations of cloud-free LST ( $^{\circ}\text{C}$ ) at SURFRAD stations  $Y_1(t)$ , and systematic differences in expected values  $Y_2(t) - Y_1(t)$ ,  $Y_3(t) - Y_1(t)$ ,  $Y_3(t) - Y_2(t)$  of LST observed at SURFRAD stations (1), GOES-8 (2), and GOES-10 (3) satellites. Negative values are shaded. Dashed lines display sunrise and sunset times.

view of downward looking pyrgeometers at SURFRAD stations is given by *Augustine et al.* [2000].

[15] The  $a_{00}$  coefficient in approximation (2) gives us an estimate of the annual mean clear-sky LST. Such 2001

annual means for observations of LST at selected SURFRAD stations and from two GOES satellites are given in Table 1. Differences between these independently observed annual mean values of LST at a single station are as high as

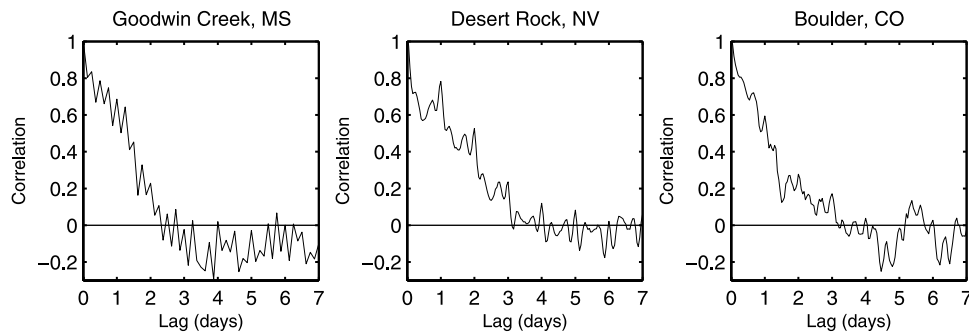


**Figure 2.** Empirical estimates of Lag-correlation function of weather-related component in GOES-10 observed clear-sky LST in vicinity of three SURFRAD stations.

2.0°C. Our assumption is that some of these differences are due to physical differences in the footprints of the radiometers and are not necessarily caused by systematic errors of observations.

[16] The estimates of time-dependent expected value  $Y_i(t)$  contain all systematic errors, including LST retrieval errors, effects of differences in the footprints, and angular anisotropy of observed land surface temperature. The effect of angular anisotropy can be diminished by using nighttime observations. The last three columns of Table 1 show mean differences of nighttime observed LST for the same selected locations. We see that GOES-8 nighttime observed LST averages  $\sim 0.6^\circ\text{C}$  warmer than GOES-10 observed LST. SURFRAD-observed LST is  $\sim 0.5^\circ\text{C}$  warmer when compared to GOES-8 and  $\sim 1.1^\circ\text{C}$  warmer when compared to GOES-10 observed LST. Such systematic differences cannot be neglected. An assumption based on common sense can be made. For example, let us assume that nighttime LST observation at the set of five selected SURFRAD stations is conditionally unbiased. Under this assumption all GOES-8 observed LST could be corrected by adding a constant bias of  $0.5^\circ\text{C}$ , and all GOES-10 observed LST should be corrected by adding a constant bias of  $1.1^\circ\text{C}$ . The main advantage of such a decision is that the same SURFRAD stations are going to continue their observation in the future and will be available for evaluation of constant biases in LST observation from future generations of GOES satellites and with future algorithms for LST retrieval. Unfortunately, estimates of the nighttime biases in LST are not very stable and vary from station to station. A much larger set of land-based stations should be used to obtain acceptable correction coefficients.

[17] As soon as  $Y_2(t)$  and  $Y_3(t)$  are estimated, up to 15 min lag between times of “coincided” observation of two satellites can be taken into account in computation of standard errors of observation from (5). The estimates of standard errors of clear-sky LST observations  $\delta_1$ ,  $\delta_2$ ,  $\delta_3$  are given in Table 1. None of these errors exceeds  $1.3^\circ\text{C}$ . Standard errors of LST observation at SURFRAD stations are very close to those for GOES satellites. These errors are relatively small and estimated correlation coefficients  $r_{ij}$  between residuals  $y_i(t) - Y_i(t)$  and  $y_j(t) - Y_j(t)$  exceed 0.9 (Table 1).

#### 4.3. Weather-Related Variations

[18] This component of LST variability by definition (3) is the same for data observed at a SURFRAD station, and

satellites GOES-8 and GOES-10. Standard deviations of LST as estimated from (6) for locations of selected SURFRAD stations are given in Table 1. They are found to be in the range from 3 to  $5^\circ\text{C}$  and are significantly larger than the standard errors of observation.

[19] The empirically estimated lag-correlation functions (7) of weather-related variations of clear-sky LST obtained from the 2001 GOES-10 observations at the locations of three SURFRAD stations are shown in Figure 2. These lag-correlation functions are almost identical to each other and have an autocorrelation radius of about  $\sim 3$  days. Analysis shows that the ignored higher harmonics of the seasonal and diurnal cycle do not change this estimate noticeably. Such a radius of autocorrelation is typical for meteorological variables with weather-related scales of variability. Small fluctuations of the estimates of autocorrelation functions are related to sampling errors, gaps in observations, imperfection of the mathematical model (2), and to neglected diurnal and seasonal cycles of variance and correlations.

[20] We can conclude that weather-related component  $y'(t)$  of clear-sky LST can be successfully monitored by GOES satellites with random errors which are relatively small compared to the signal. This variable has no diurnal cycle and can be displayed as a map for each time of satellite observation. However, a large preliminary work on evaluation of time-dependent expected value  $Y(t)$  for each satellite and each pixel is required to accurately compute differences  $y'(t) \approx y(t) - Y(t)$ .

#### 5. Concluding Remarks

[21] Using a single year of observations we can obtain the reference-year estimate of  $Y(t)$  that is only an approximate estimate of real expected value. There are some problems with using this reference  $Y(t)$  estimates for computation of  $y'(t)$  for observations beyond the reference year. In such a case interannual variability and long-term trends are part of the temporal variation of  $y'(t)$ , which should be interpreted as the weather- and climate-related anomaly of LST. Such an approach can be utilized for long-term climate change monitoring.

[22] The other problem is that satellite observed LST cannot be made with infrared sensors under cloudy sky conditions, but only in clear-sky conditions. Cloud-caused observation gaps cannot be filled by interpolation or extrapolation in time and space. It is not clear if temporal or spatial averaging of clear-sky data can be applied to extend coverage to cloud-covered areas.

[23] GOES satellites provide no information on LST under cloudy skies. But, observation of land-based stations, SURFRAD and Climate Reference Network (CRN) among them, can be used to empirically study the effect of cloudiness on LST. This should be done before it will be possible to assimilate satellite-retrieved LST information into operational weather data analysis systems.

[24] Real-time validation of GOES-observed LST can be based on comparison of weather-related anomalies in LST computed from observations at surface stations and the two GOES satellites. The differences between three independent estimates of weather-related anomalies are expected to be random and their standard errors should not exceed permitted limits. These errors should be monitored routinely and continuously. Systematic differences in LST observed by two satellites and surface stations are expected to be stable in time. Their evolution should be monitored and analyzed periodically.

[25] Angular anisotropy of LST for satellite observations is a real physical phenomenon. Systematic differences of LST observed by two geostationary satellites and SURFRAD stations are a manifestation of this anisotropy. We suggest that SURFRAD-type pyrgeometric observations of LST be used as ground truth and as a basis for definition of this physical variable. Good parameterization of the angular dependence of LST on physical parameters of land surface, solar and satellite angles is needed if we want to work with real temperatures, not with anomalies. But it can be expected that climatic trends with their diurnal-seasonal cycles may be much less affected by the angular anisotropy. In such a case, the trend term should not be excluded from analytical expression used to approximate time-dependent expected values in multi-year observations of temperature [Vinnikov *et al.*, 2004, 2006].

[26] **Acknowledgments.** We thank NESDIS/NOAA GOES-R AWG for supporting this work through a research grant to CICS; Istvan Laszlo, Marco Vargas, Larry Flynn, Norman Grody and the reviewers for valuable comments. The manuscript contents are solely the opinions of the authors and do not constitute a statement of policy, decision, or position on behalf of NOAA or the U. S. Government.

## References

- Augustine, J. A., J. J. DeLuisi, and C. N. Long (2000), SURFRAD-A national surface radiation budget network for atmospheric research, *Bull. Am. Meteorol. Soc.*, *81*, 2341–2357.
- McMillin, L. M. (1975), Estimation of sea surface temperatures from two infrared window measurements with different absorption, *J. Geophys. Res.*, *80*, 5113–5117.
- McMillin, L. M., and D. S. Crosby (1984), Theory and validation of multiple window sea surface temperature technique, *J. Geophys. Res.*, *89*, 3655–3661.
- Minnis, P., and M. M. Khaiyer (2000), Anisotropy of land surface skin temperature derived from satellite data, *J. Appl. Meteorol.*, *39*, 1117–1129.
- Rama Varma Raja, M. K., Y. Yu, D. Tarpley, H. Xu, and K. Y. Vinnikov (2008), The manual cloud filtering of GOES-satellite data through combined use of satellite and ground measurements, paper presented at Fifth GOES Users' Conference, Am. Meteorol. Soc., New Orleans.
- Schmit, T. J., M. M. Gunshor, W. P. Menzel, J. J. Gurka, J. Li, and A. S. Bachmeir (2005), Introducing the next generation Advanced Baseline Imager on GOES-R, *Bull. Am. Meteorol. Soc.*, *86*, 1079–1096.
- Snyder, W. C., Z. Wan, and Y. Z. Feng (1998), Classification-based emissivity for land surface temperature measurement from space, *Int. J. Remote Sens.*, *19*, 2753–2774.
- Olivieri, C., and G. Cannizzaro (1985), Land surface temperature retrievals from satellite measurements, *Acta Astronaut.*, *12*, 985–997.
- Vinnikov, K. Y., and N. C. Grody (2003), Global warming trend of mean tropospheric temperature observed by satellites, *Science*, *302*, 269–272.
- Vinnikov, K. Y., A. Robock, N. C. Grody, and A. Basist (2004), Analysis of diurnal and seasonal cycles and trends in climatic records with arbitrary observation times, *Geophys. Res. Lett.*, *31*, L06205, doi:10.1029/2003GL019196.
- Vinnikov, K. Y., N. C. Grody, A. Robock, R. J. Stouffer, P. D. Jones, and M. D. Goldberg (2006), Temperature trends at the surface and in the troposphere, *J. Geophys. Res.*, *111*, D03106, doi:10.1029/2005JD006392.
- Yu, Y., D. Tarpley, J. L. Privette, M. D. Goldberg, M. K. Rama Varma Raja, K. Vinnikov, and H. Xu (2008), Developing algorithm for operational GOES-R land surface temperature product, *IEEE Trans. Geosci. Remote Sens.*, *46*(12).
- M. D. Goldberg, D. Tarpley, and Y. Yu, National Environmental Satellite, Data, and Information Service Center for Satellite Applications and Research, NOAA, 5200 Auth Road, World Weather Building, Camp Springs, MD 20746, USA.
- M. K. Rama Varma Raja, I. M. Systems Group, Inc., NOAA/NESDIS/STAR, World Weather Building, 5200 Auth Road, Camp Springs, MD 20746, USA.
- K. Y. Vinnikov, Department of Atmospheric and Oceanic Science, University of Maryland, College Park, MD 20742, USA. (kostya@atmos.umd.edu)